THE ASTROPHYSICAL JOURNAL, 550:383–391, 2001 March 20

VACUUM GAPS IN PULSARS AND PSR J2144−3933

JANUSZ GIL[1] AND DIPANJAN MITRA[2]
Received 2000 June 1; accepted 2000 November 11

ABSTRACT

In this paper we revisit the radio pulsar death line problem within the framework of curvature radiation and/or the inverse Compton scattering–induced vacuum gap model above neutron star polar caps. Our special interest is in the recently detected pulsar PSR J2144−3933 with extremal period 8.5 s, which lies far beyond conventional death lines. We argue that the formation of vacuum gaps requires a complicated multipolar surface magnetic field, with a strength B_s typically much higher than the surface dipolar component B_d and a radii of curvature $\mathscr{R}$ much smaller than the neutron star radius $R = 10^6$ cm. Such a multipolar surface field is also consistent with death lines including the extremal pulsar PSR J2144−3933. Since vacuum gap models produce sparks, our paper naturally supports the spark related models of subpulse drift phenomenon as well as the spark-associated models of coherent pulsar radio emission.

Subject headings: magnetic fields — pulsars: general — pulsars: individual (J2144−3933) — radiation mechanisms: nonthermal

1. INTRODUCTION

Radio pulsars are believed to turn off when they can no longer produce electron-positron pairs in strong and curved magnetic fields within a so-called inner accelerator region just above the polar cap. The limiting rotational period P at which this occurs depends on the magnitude and configuration of the surface magnetic field B_s. Unfortunately, only the dipolar component B_d of this field can be deduced from the observed spin-down rate. The line on the B_d-P plane or $\dot{P}$-P plane corresponding to this critical period is called a death line. No radio pulsar should be observed to the right or below this line, i.e., with a period longer than the critical one. Recently, Young, Manchester, & Johnston (1999) reported on the existence of PSR J2144−3933 with a period of 8.5 s, which is by far the longest known. This pulsar, which is located far beyond all conventional death lines, seems to challenge existing emission models. As Young et al. (1999) concluded themselves, under the usual assumptions, this slowly rotating pulsar should not be emitting a radio beam.

In this paper we attempt to examine this problem assuming that PSR J2144−3933 generates radio emission just the same way as other pulsars. Assuming that the pulsar's inner accelerator is the vacuum gap (VG) driven by curvature radiation (CR) for pair production in strong magnetic fields, we find that its radio detection is consistent with a strong and complicated surface magnetic field in pulsars. When such fields with a magnitude much greater than the measurable dipole component and a radius of curvature much smaller than the neutron star radius $R = 10^6$ cm are assumed, then one can easily find general death lines which include PSR J2144−3933 on their left-hand side (see Fig. 1). This is consistent with Arons & Scharlemann (1979), who noted that if pair creation is essential for coherent radio emission, then pulsars with very long periods (~ 5 s) require a more complex surface field than a pure dipole (see also Arons 2000, where similar conclusions were drawn in a more complete treatment, including inverse Compton scattering [ICS] as a source of pairs and a frame-dragging effect modifying the electric field near the polar cap surface). We demonstrate in this paper that the formation of a vacuum gap above the pulsar polar cap is possible, provided that the surface magnetic field is extremely nondipolar (sunspot-like).

Young et al. (1999) in their discovery paper already noticed that an extremely curved and strong surface field would solve the problem of a death line in PSR J2144−3933. They were reluctant however to accept that such an extreme configuration with $B_s \gg B_d$ and $\mathscr{R} \ll R$ could exist. Zhang, Harding, & Muslimov (2000) argued that if the pulsar's inner accelerator is the so-called space charge limited flow (SCLF) with the ICS as the dominating mechanism of pair production, then a pure dipolar magnetic field configuration is sufficient to produce death lines that can explain the presence of this pulsar. We, however, for reasons explained below, will assume that the surface magnetic field configuration required by the curvature-radiation–induced vacuum gap (VG-CR) and/or inverse Compton scattering–vacuum gap (VG-ICS) is just what nature creates in pulsars, which perhaps is not the simplest explanation but nevertheless a possibility, which we intend to explore in this paper.

The only strong condition to define pulsar death lines is the condition for pair production, regardless of the detailed mechanisms to produce these pairs. Pulsar death lines therefore are model dependent. In history, both the VG model and the SCLF model have been developed, and the corresponding death lines of both models were investigated by Ruderman & Sutherland (1975, hereafter RS75) and Arons & Scharlemann (1979). The original versions of both models assume CR to be the dominating mechanism for pair production and neglect the influence of the general relativistic frame-dragging effect and other sources of pairs. Both models were later improved to include the frame-dragging effect (Muslimov & Tsygan 1992) and the ICS (Zhang, Qiao, & Han 1997a; Zhang et al. 1997b) as an alternative mechanism for pair production. Zhang et al.

[1] Johannes Kepler Astronomical Center, Lubuska 2, 65-265 Zielona Góra, Poland; jag@astro.ca.wsp.zgora.pl.
[2] Raman Research Institute, C. V. Raman Avenue, Bangalore 560080, India. Present address: Inter University Center for Astronomy and Astrophysics, Post Bag 4, Ganeshkhind, Pune 411007, India; dmitra@iucaa.ernet.in.

(2000) fully investigated death lines of all different kinds of models. In § 2 we argue that both the observational data and the theory of coherent radio emission seem to favor the VG models of an inner pulsar accelerator. We find that the group of pulsars with drifting subpulses can be explained naturally by the VG-CR model, but to explain all the normal pulsars one also has to invoke the VG-ICS model.

2. THE INNER ACCELERATOR AND OBSERVED PULSAR RADIO EMISSION

As mentioned above, two types of the polar cap acceleration models (VG and SCLF) usually are considered. In the VG models, the free outflow of charges from the polar cap is impeded, and the high-acceleration potential drop is related to the formation of an empty gap above the polar cap (Sturrock 1971; RS75; Cheng & Ruderman 1977, 1980). In the SCLF models, the charged particles flow freely from the polar cap surface and accelerate within a height scale of about 1 $R_\star$, $R = 10^6$ cm, because of the potential drop resulting from the curvature of magnetic field lines and/or inertia of outstreaming particles (Arons & Scharlemann 1979; Arons 1993). Although this potential drop is too weak to explain the entire population of existing radio pulsars, Muslimov & Tsygan (1992) have shown that the relativistic effect of inertial frame dragging generates an additional potential drop within about 1 stellar radius, which is almost 2 orders of magnitude larger than the inertial potential drop. In both the VG and SCLF models, either the CR or the ICS photons should be considered as the sources of pairs.

It is well known that the VG models suffer from the so-called binding-energy problem (see, e.g., Hillebrandt & Müller 1976; Kössl et al. 1988). It was demonstrated that the binding energy of ^{56}Fe ions is much too small to prevent thermionic emission from the surface, and thus formation of a vacuum gap above the pulsar polar cap was questionable. Thus, the binding-energy problem is an important difficulty of the VG models, and, in this sense, the SCLF models are more natural, unless some further assumptions are adopted and justified. Xu, Qiao, & Zhang (1999; for review see Xu et al. 2000) proposed that pulsars showing drifting subpulses, thus requiring some kind of VG inner accelerator, are bare polar cap strange stars (BPCSSs) rather than neutron stars. This attractive but exotic conjecture is based on the argument that the work function for both electrons and positrons in BPCSSs is practically infinite. In this paper we argue that the binding-energy crisis can be solved alternatively and more naturally by assuming an extremely strong and curved surface magnetic field above the neutron star polar cap. Therefore, we conclude that invoking the BPCSS conjecture is not necessary.

An important feature that distinguishes VG models from SCLF models is that the former produce sparks, as originally delineated by RS75. Each spark generates a plasma cloud, and the interaction of adjacent clouds may have something to do with the generation of coherent radio emission (see below). Because of $\boldsymbol{E} \times \boldsymbol{B}$ drift within the gap, the subpulse-associated sparks are expected to rotate slowly around the magnetic pole, at a rate which can be tested observationally in pulsars showing drifting subpulses in their single pulse emission. Recently, Deshpande & Rankin (1999) analyzed drifting subpulses in PSR B0943+10 with a newly developed technique called "cartographic transform," based on the sophisticated fluctuation spectra analysis. They obtained a clear map of the polar cap with 20 sparks rotating around the pole at the rate consistent with the RS75 model, with each spark completing one full rotation in 37 pulsar periods. It is this consistency which tells us that the RS75-type VG model is realized in nature, at least in pulsars showing periodicities in their fluctuation spectra that can be associated with rotating sparks. It is important to emphasize that it is not just a handful a pulsars with clearly drifting subpulses. Rankin (1986) demonstrated that such periodicities in the 2–15 pulsar period range are common among the so-called conal profile components, while core components either do not show any evidence of periodicities or they are much weaker (in the 15–50 pulsar period range). In Figure 1 we marked by crossed circles 41 pulsars showing periodic subpulse modulations, following Rankin (1986, Tables 2 and 3).

Gil & Sendyk (2000) reanalyzed the case of PSR B0943+10 and three other pulsars with a clear subpulse drift (Table 1) within their modified RS75 model. They confirmed the consistency of the observed periodicities with their modified RS75 VG model. The fundamental drift periodicity can be expressed by $P_3 \approx Pa^2/N$, where $a = r_p/h$ (the complexity parameter) is the ratio of the canonical polar cap radius to the gap height, P is the pulsar period, and N is the number of sparks circulating around the pole. For PSR B0943+10, $a \approx 6$, $N = 20$, and therefore $P_3 \approx 1.8P$, as observed (see, e.g., Deshpande & Rankin 1999). For small values of a, $P_3 < 2P$, and the subpulse drift is hard to detect. For medium values of a, the P_3 values are in the range (2–15)P, and for very large $a \gg 10$ (core single pulsars; see Gil & Sendyk 2000), the P_3 periods largely exceed 15P.

The fundamental problem of pulsar studies is that there is no consensus at all about the radio emission mechanism except that pair production is an essential condition and that the radiation mechanism must be coherent. Yet another widely accepted constraint is that the emission region is located close to the neutron star, at altitudes roughly a few percent of the light cylinder radius $R_{\rm LC} = cP/2\pi$ (Cordes 1992; Kijak & Gil 1997). However, in the millisecond pulsars it can reach even $\sim$30% of $R_{\rm LC}$ (Kijak & Gil 1998).

After more then 30 yr of intensive research, only a few successful, self-consistent models of the generation of coherent pulsar radio emission can be found in the literature. Historically, the first one (called the Georgian model) was proposed by Kazbegi et al. (1987) and Kazbegi, Machabeli, & Melikidze (1992). In this model, based on the SCLF inner acceleration scenario, the radio emission is generated by a maser relativistic plasma radiation. This model requires a relatively low magnetic field, thus high emission altitudes (larger than 30% of $R_{\rm LC}$), and therefore its possible applicability is restricted to millisecond pulsars.

Qiao & Lin (1998; for a review, see Xu, Zhang, & Qiao 2001) proposed a coherent ICS model of pulsar radio emission. This model is based on the sparking VG scenario (Xu et al. 2001). The low-frequency electromagnetic wave associated with development and decay of a spark is scattered on bunches of outstreaming particles. The coherent ICS model seems to have some observational difficulties. As Xu et al. (2001) argued, it can reproduce the core pulsar beam and two conal (inner and outer) beams. However, present-day observational data suggest that pulsar beams may consist of up to three or even four nested cones (Mitra & Deshpande

1999; Gil & Sendyk 2000), which cannot be explained within the ICS model. The more serious problem is the observed pulsar polarization. The coherent ICS model predicts that the individual emission corresponding to the core beam should be circularly polarized, while the conal beams should demonstrate no significant circular polarization (Xu et al. 2001). However, available polarimetric observations of single pulses show that subpulses in conal pulsars are clearly circularly polarized, with sense reversals near the subpulse and/or micropulse peak (Gil 1992; Gangadhara et al. 1999). This property, if confirmed in a larger sample of pulsars, might be a big challenge for the coherent ICS model of pulsar radio emission. The same applies to the maser relativistic plasma radiation (Georgian model).

Recently, a new idea has been developed, according to which the observed pulsar radio emission is a coherent curvature radiation emitted by charged solitons associated with sparks operating in the inner VG accelerator (Asseo & Melikidze 1998; Gil & Sendyk 2000; Melikidze, Gil, & Pataraya 2000). The model is entirely self-consistent and determines pulsar characteristics by two basic observables, P and $\dot{P}$. The present version of the soliton model explores the VG-CR model, although the VG-ICS alternative is not excluded.

Pulsars with drifting subpulses, which require the existence of sparks, are distributed more or less uniformly over the bulk of typical pulsars on the P-$\dot{P}$ diagram (Fig. 1). On the other hand, radio emission of typical pulsars originates at low altitudes, which favors radiation models based on the sparking scenario. It is thus clear from the above discussion that the VG-CR and/or VG-ICS models seem to be preferred in typical pulsars, from both the observational and theoretical point of view. We therefore concentrate in this paper on this class of inner accelerator models, and we plan to give a full treatment, including the SCLF along with the frame-dragging effect (which perhaps can be applied to millisecond pulsars), in a separate paper.

3. VACUUM GAP FORMATION IN A SUPERSTRONG MAGNETIC FIELD

We will argue in this paper that the actual surface magnetic field is extremely strong and curved with $B_s \gg B_d$ and $\mathcal{R} \ll R$, where $B_d = 6.4 \times 10^{19}(P\dot{P})^{1/2}$ G is the global surface dipole component (see, e.g., Zhang & Harding 2000a), $\mathcal{R}$ is the radius of curvature of surface field lines, and $R = 10^6$ cm is the neutron star radius. Thus, for a convenience of further considerations, we present in this section new results concerning gap formation and death lines in superstrong magnetic fields, $B_s > 0.1B_q$, where $B_q = m^2c^3/e\hbar = 4.4 \times 10^{13}$ G is the critical magnetic field strength at which the electron gyrofrequency $\hbar\omega_c = \hbar eB/mc$ is equal to its rest mass. Above this strength the photon-splitting phenomenon may inhibit the pair formation process (Baring & Harding 1998). More exactly, the photon splitting becomes effective above the critical field strength $B_c \simeq (5.7 \times 10^{13}\ \mathrm{G})P^{2/5}$ (see, e.g., Zhang & Harding 2000b).

In the superstrong magnetic field $B > 0.1B_q \approx 5 \times 10^{12}$ G, the high-energy photons with frequency ω will produce electron positron pairs at or near the kinematic threshold (see, e.g., Daugherty & Harding 1983):

$$\hbar\omega = 2mc^2/\sin\theta\ , \quad (1)$$

where $\sin\theta = l_{\rm ph}/\mathcal{R}$, $l_{\rm ph}$ is the photon mean free path for pair formation, and $\mathcal{R} = \mathcal{R}_6 \times 10^6$ cm the radius of curvature of magnetic field lines within the gap. The typical photon energy is

$$\hbar\omega = (3/2)\hbar\gamma^3 c/\mathcal{R} \quad (2)$$

in the case of curvature radiation (see, e.g., RS75), and

$$\hbar\omega = 2\gamma\hbar eB/mc \quad (3)$$

in the case of the resonant inverse Compton scattering (see, e.g., Zhang et al. 1997a). Here γ is the typical Lorentz factor, $\hbar$ is the Planck constant, m is the electron mass, e is the electron charge, and c is the speed of light. It is worth emphasizing that the near-threshold gap parameters have not been studied before.

3.1. *Curvature Radiation Induced Near-Threshold Vacuum Gaps*

Let us consider the CR photons as sources of pairs first. The gap height h is determined by the condition $h = l_{\rm ph}$. The Lorentz factor γ can be calculated from the potential drop across the gap:

$$\Delta V = (2\pi/cP)B_s h^2 \text{ as} \quad (4)$$

$$\gamma = \frac{e\Delta V}{mc^2}\ . \quad (5)$$

If we express the surface magnetic field as $B_s = bB_d = 2b(P\dot{P}_{-15})^{1/2}$, then equations (1), (2), (4), and (5) give the gap height in the form

$$h = (3 \times 10^3)\mathcal{R}_6^{2/7} b^{-3/7} P^{1/7} \dot{P}_{-15}^{-1/7}\ \text{cm}\ , \quad (6)$$

where $0.1B_q < b < B_q/B_d$ and $\mathcal{R}_6 \lesssim 1$ ($B_q = 4.4 \times 10^{13}$ G). This can be compared with the asymptotic case (Erber 1966) valid for $B \leq 0.1B_q$:

$$h_{\rm RS} = (3.5 \times 10^3)\mathcal{R}_6^{2/7} b^{-4/7} P^{-1/7} \dot{P}_{-15}^{-2/7}\ \text{cm}\ , \quad (7)$$

where $b \gtrsim 1$ and $\mathcal{R}_6 \sim 1$ (RS75).

To obtain the critical lines for the VG formation, we use the condition $T_s/T_i \leq 1$, where the ion critical thermonic temperature above which ^{56}Fe ions will not be bound is

$$T_i = 10^7(B_s/10^{14}\ \mathrm{G})^{0.73} \approx (6 \times 10^5) b^{0.73} (P\dot{P}_{-15})^{0.36}\ \mathrm{K} \quad (8)$$

(Abrahams & Shapiro 1991; Usov & Melrose 1995; Zhang & Harding 2000b), and the actual surface temperature is

$$T_s = (\kappa\mathcal{F})^{1/4}\left(\frac{e\Delta V\dot{N}}{\sigma\pi r_p^2}\right)^{1/4}\ , \quad (9)$$

where $\dot{N} = \pi r_p^2 B_s/(eP)$ is the particle flux through the polar cap with radius $r_p = (1.4 \times 10^4) b^{-0.5} P^{-0.5}$ cm, ΔV is expressed by equation (4), and the reduction parameters $\kappa \approx \mathcal{F} \lesssim 1$ are described in § 4. The family of critical lines for VG-CR formation in the superstrong and extremely curved surface magnetic field therefore has a form

$$\dot{P}_{-15} = 2.7 \times 10^3 (\kappa\mathcal{F})^{1.15} \mathcal{R}_6^{0.64} b^{-2} P^{-2.3}\ , \quad (10)$$

with actual lines depending on the values of parameters b and $\mathcal{R}_6$ (as well as κ and $\mathcal{F}$). The curvature-radiation–induced vacuum gap can form in pulsars lying above these lines. The parameter space for the VG-CR inner accelerator is approximately determined by the two extremal lines corresponding to $(\kappa\mathcal{F})^{1.15}\mathcal{R}_6^{0.64} \approx 0.1$ and $b \approx B_q/B_d$ for the lower line and $(\kappa\mathcal{F})^{1.15}\mathcal{R}_6^{0.64} \approx 1$ and $b \approx 0.1B_q/B_d$ for the upper line.

The pulsar death line can be defined (see, e.g., RS75) by the condition that the actual potential drop across the gap accelerator, $\Delta V = (2\pi/cP)Bh^2$ (eq. [4]), required to produce enough pairs per primary to screen out the gap electric field is larger than the maximum potential drop $\Delta V_{\rm max} = (2\pi/cP)bh^2_{\rm max}$ available from the pulsar, in which case no secondary pairs will be produced. Since $h_{\rm max} = r_p/\sqrt{2}$ (RS75), where $r_p = 1.4b^{-0.5}10^4P^{-0.5}$ cm is the polar cap radius, then, using equation (6) for the gap height $h = h_{\rm max}$, we obtain family–of–death line equations for the VG-CR in the form

$$\dot{P}_{-15} = (2.4 \times 10^{-4})\mathscr{R}_6^2 b^{0.5}P^{4.5} . \qquad (11)$$

All pulsars driven by the VG-CR inner accelerator should lie to the left of these lines on the P-$\dot{P}$ diagram if the surface magnetic field is stronger than about 5×10^{12} G. The extremal line is determined by a maximum value of $b \sim B_q/B_d$ and a minimum value of $\mathscr{R}_6 \sim 0.1$.

3.2. *Inverse Compton Scattering–induced Near-Threshold Vacuum Gaps*

In this case we have to consider the mean free path l_e of an electron/positron moving with Lorentz factor γ to emit one photon with energy expressed by equation (3), since $l_e \sim 0.00276\gamma^2B_{12}^{-1}T_6^{-1} \sim l_{\rm ph}$ (Zhang et al. 2000), while $l_e \ll l_{\rm ph}$ in the CR case. Here $B_{12} = 2b(P\dot{P}_{-15})^{1/2}$, and T_6 is the surface temperature in units of MK. Thus, assuming that $l_{\rm ph} \sim l_e$, we obtain from equations (1) and (3) the typical Lorentz factors $\gamma = (2.2 \times 10^7)h^{-1}\mathscr{R}_6 b^{-1}(P\dot{P}_{-15})^{-0.5}$. The surface temperature obtained from equation (9) is $T_6 = T/10^6$ K $= 0.06b^{0.5}h^{0.5}\dot{P}_{-15}^{0.25}P^{-0.25}$, and the electron mean free path $l_e \approx 10^{13}\mathscr{R}_6^2 b^{-3.5}h^{-2.5}P^{-1.25}\dot{P}_{-15}^{-1.75}$. Now setting $h = l_{\rm ph} = l_e$ (Zhang et al. 2000), we can find the ICS-induced near-threshold ($B > 5 \times 10^{12}$ G) gap height:

$$h = (5 \times 10^3)\mathscr{R}_6^{0.57}b^{-1}P^{-0.36}\dot{P}_{-15}^{-0.5} \text{ cm} , \qquad (12)$$

where $b \gg 1$ and $\mathscr{R}_6 \ll 1$. This h can be compared with the asymptotic case ($B < 5 \times 10^{12}$ G) given by Zhang et al. (2000):

$$h = (8.8 \times 10^3)\mathscr{R}_6^{0.57}b^{-1.57}P^{-0.64}\dot{P}_{-15}^{-0.79} \text{ cm} , \qquad (13)$$

where $b \gtrsim 1$ and $\mathscr{R} \sim 1$.

Now, getting back to the surface temperature expressed in terms of h, we obtain

$$T_s = 4 \times 10^6(\kappa\mathscr{F})^{0.25}\mathscr{R}_6^{0.28}P^{-0.43} \text{ K} . \qquad (14)$$

The gap condition $T_s/T_i = 7\mathscr{R}_6^{0.28}b^{-0.73}P^{-0.79}\dot{P}_{-15}^{-0.36} \leq 1$ gives the family of critical lines

$$\dot{P}_{-15} = 2 \times 10^2(\kappa\cdot\mathscr{F})^{0.7}\mathscr{R}_6^{0.8}b^{-2}P^{-2.2} , \qquad (15)$$

with actual lines depending on values of parameters b and $\mathscr{R}_6$ (as well as on κ and $\mathscr{F}$). The ICS-induced vacuum gap in a strong magnetic field, $B > 5 \times 10^{12}$ G, can form in pulsars lying above these lines as long as $B < B_q \sim 5 \times 10^{13}$ G.

To obtain a death line for the near-threshold VG-ICS, we need to equate the gap height expressed by equation (12) to $r_p/\sqrt{2}$, which leads to family of lines

$$\dot{P}_{-15} = 0.25\mathscr{R}_6^{1.14}b^{-1}P^{0.28} . \qquad (16)$$

All pulsars driven by a strong-field ($B > 5 \times 10^{12}$ G) VG-ICS inner accelerator should lie above these lines on the P-$\dot{P}$ diagram.

4. BINDING-ENERGY PROBLEM AND VACUUM GAPS IN PULSARS

As discussed above, recent analysis of drifting subpulses in pulsars (Deshpande & Rankin 1999; Vivekanand & Joshi 1999; Gil & Sendyk 2000) strongly suggests that sparks rotating around the magnetic pole in a vacuum gap do exist, at least in some pulsars. Such a scenario was first proposed by RS75, but then it was criticized because of the so-called binding-energy problem. However, the binding-energy calculations were made under the assumption of a global dipolar magnetic field above the polar cap. Here we discuss an influence of strong multipolar components dominating the surface field on the formation of a vacuum gap above the neutron star polar caps.

Let us begin with a standard approach based on the classical work of RS75. Within the vacuum gap, the high potential drop discharges via a number of isolated sparks. This number is roughly equal to a^2, where $a = r_p/h$ is the so-called complexity parameter, $r_p = 10^4P^{-1/2}$ cm is the canonical polar cap radius, and h is the polar gap height, which is also the spark characteristic dimension (Gil & Sendyk 2000). The effective surface area beneath a^2 sparks in a strong surface magnetic field, $B_s = bB_d$, is $A_{\rm eff} \approx a^2\pi(h/2)^2 = \pi 10^8/(4bP) = A_{\rm GJ}/(4b)$, where $A_{\rm GJ}$ is the canonical area of the Goldreich-Julian (1969) polar cap with a dipolar field. The maximum back-flow current of electrons (positrons) heating the polar cap beneath sparks is $I_{\rm max} = e\dot{N}_{\rm max}/(4b)$, where $\dot{N}_{\rm max}$ is the maximum available flux density corresponding to final stage of development of the spark's plasma (eq. [1] in RS75). At this stage the potential drop beneath the spark is $\Delta V = \mathscr{F}V_{\rm RS}$, where $V_{\rm RS}$ is the vacuum gap potential drop (see eq. [23] of RS75), and $\mathscr{F} < 1$ is the reduction factor describing the voltage discharge at final stages of the spark-developing process. The parameter $\mathscr{F} = 1$ only in the empty gap, but when a sparking avalanche develops, its value should drop significantly below unity (vacuum value). In fact, when a spark ignites, its first shower deposits very few charges at the gap boundaries, and the voltage across the gap is almost the maximum vacuum value. But a few microseconds later the shower flux density reaches maximum value, and the gap voltage beneath the spark is reduced significantly to values inhibiting further effective pair production (Gil & Sendyk 2000). At this stage heating is much more effective than at the very beginning of the spark discharge. Moreover, this effective heating stage is not reached at the same time in all adjacent sparks. We therefore will introduce below a "heating efficiency" factor $\kappa < 1$. The energy deposited by cascading charges onto the polar cap surface will diffuse into deeper layers of the crust and diffuse out in a later time (see, e.g., Eichler & Cheng 1989). Some heat may not be transferred back to be reemitted from the surface. We will make all calculations for $\mathscr{F} \approx \kappa \approx 1$ and discuss a possibility that both these parameters are slightly lower than unity.

The thermal X-ray flux from the polar cap populated with a^2 sparks is $L_x = \kappa\Delta VI_{\rm max} = \kappa\mathscr{F}\dot{E}_x/(4b)$, where $\dot{E}_x = 10^{30}b^{6/7}B_{12}^{6/7}\mathscr{R}_6^{4/7}P^{-15/7}$ ergs s^{-1} is the upper bound for the energy flux carried by relativistic positrons into the magnetosphere above the gap (see eq. [26] of RS75). Since $L_x = A_{\rm eff}\sigma T_s^4$, where $\sigma = 5.7 \times 10^{-5}$ cm^{-2} K^{-4} ergs s^{-1}, we obtain an estimate of the actual surface temperature $T_s \approx 3(\kappa\mathscr{F})^{0.25}10^6b^{0.21}\mathscr{R}_6^{0.14}\dot{P}_{-15}^{-0.43}P^{0.14}$ K. The iron critical temperature T_i above which the ^{56}Fe ions will not be bound

TABLE 1

FOUR PULSARS WITH CLEARLY DRIFTING SUBPULSES

PSR	P (s)	$\dot{P}_{15}$	$L_X/10^{30}$ (ergs s^{-1})	T_s (10^6 K)	T_i (10^6 K)
0031−07......	0.94	0.4	0.012	2.2	2.2
0943+10......	1.1	3.5	0.027	2.8	5.0
2303+30......	1.57	2.9	0.014	2.4	5.6
2319+60......	2.26	7.0	0.013	2.3	8.7

is described by equation (8). Using the ratio of the surface, T_s, and ion, T_i, temperatures

$$T_s/T_i \approx 5(\kappa\mathscr{F})^{0.25} b^{-0.52} \mathscr{R}_6^{0.14} P^{-0.22} \dot{P}_{-15}^{-0.79} , \quad (17)$$

we can write a condition for the formation of a vacuum gap $T_s/T_i \lesssim 1$ in the form

$$\dot{P}_{-15} > 7.7(\kappa\mathscr{F})^{0.32} b^{-0.66} \mathscr{R}_6^{0.18} P^{-0.28} . \quad (18)$$

If we now use $\kappa\mathscr{F} = 1$, $\mathscr{R}_6 = 1$, and a relatively high $b = 5$, then the critical line above which the VG-CR can form is $\dot{P}_{-15} > 2P^{-0.28}$. As one can see, this line marked in Figure 1 as line 1 leaves almost half of the known pulsars below it.

In an attempt to explain pulsars below line 1, let us now consider a superstrong surface magnetic field, $B_s \gg B_d$. In such a strong field, the pairs are created near the kinematic threshold $(\hbar\omega/2mc^2)(h/\mathscr{R}) \approx 1$ (Daugherty & Harding 1983). A general description of pair-creation processes in such a strong surface magnetic field for both CR- and ICS-induced gaps is presented in § 3. The near-threshold critical lines for the VG-CR formation are described by equation (10). To include a possibly large number of pulsars lying below the low-B_s asymptotic line 1, we will assume $b = 100$ (which requires $B_d \lesssim 5 \times 10^{11}$ G so that B_s does not exceed B_q) and $\mathscr{R}_6^{0.64}(k\mathscr{F})^{1.15} = 0.15$. This gives an extremal critical line $\dot{P}_{-15} = 0.04P^{-2.3}$, which is presented as line 2 in Figure 1.

Most pulsars with drifting subpulses (crossed circles in Fig. 1) then can be explained by the critical lines 1 and/or 2 corresponding to the curvature radiation dominated vacuum gaps. Table 1 presents four pulsars modeled carefully by Gil & Sendyk (2000) within their modified RS75 drift model. If we assume $\mathscr{R}_6 = 0.3$ and $b = 10$ in equation (17), then $T_s/T_i \leq 1$, so the VG-CR can form in these pulsars, although a relatively strong surface magnetic field $B_s \sim 10B_d$ is required. Such a strong magnetic field is consistent with the recently discovered longest period pulsar PSR J2144−3933, which we discuss in § 5. In § 6 we discuss

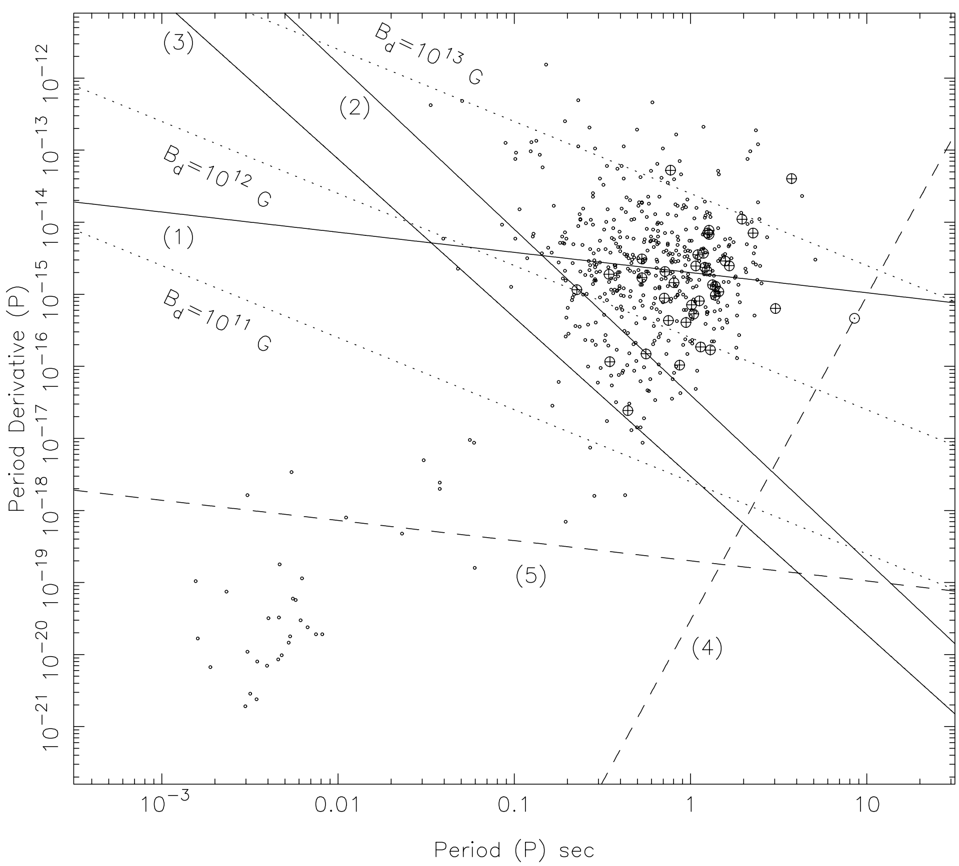

FIG. 1.—P-$\dot{P}$ diagram for 538 pulsars from the Pulsar Catalog (Taylor, Manchester, & Lyne 1993) with measured $\dot{P}$ values. The three solid lines are the critical lines for vacuum gap formation corresponding to different acceleration region models: (line 1) asymptotic VG-CR obtained from eq. (18); (line 2) near-threshold VG-CR obtained from eq. (10) for $b = 100$ and $(k\mathscr{F})^{1.15}\mathscr{R}_6^{0.64} = 0.15$; and (line 3) near-threshold VG-ICS models obtained from eq. (15) for the $b = 100$ and $(k\mathscr{F})^{0.7}\mathscr{R}_6^{0.8} = 0.1$ models, respectively. The two dashed lines represent near-threshold death lines: (line 4) obtained for CR from eq. (11) for $\mathscr{R}_6^2 b^{0.5} = 0.13$; and (line 5) obtained for ICS from eq. (16) for $b = 100$ and $\mathscr{R}_6 = 0.1$, respectively. Three dotted lines represent a constant dipole magnetic field $B_d = 10^{11}$, 10^{12}, and 10^{13} G, respectively. Pulsars with drifting subpulses are marked by crossed circles, and PSR J2144−3933 is marked by an open circle.

observational constraints for the strength of the surface magnetic multipole components and argue that strong multipole fields with $b \sim 100$ and $\mathscr{R}_6 \sim 0.1$ are well conceivable.

As one can see from Figure 1, even in the extremal case 2, quite a large number of normal pulsars lie below the critical line, meaning that the VG-CR cannot form in these objects. It is important to notice that two well-known drifting subpulse pulsars, PSRs B0820+02 and B1944+17 (Table 2 in Rankin 1986), also lie below the extremal line 2; thus, some kind of VG inner accelerator should operate in this region. We can see three possible solutions to this problem: (1) the estimation of ion critical temperature (eq. [1]) is inadequate, at least for older pulsars, (2) some radio pulsars, especially the older ones, are BPCSSs instead of neutron stars, as originally proposed by Xu et al. (1999) and Xu et al. (2001), and (3) these pulsars are driven by the VG-ICS inner accelerator. Let us briefly discuss these three possibilities. Possibility 1 is the least promising. In fact, even if the ion critical temperature T_i is underestimated by a factor of 10, one can move the critical line B down only by a factor of 18, which still leaves quite a number of normal pulsars below it. Possibility 2 would improve the situation radically, since the binding energy in bare polar caps of strange stars is almost infinite for both electrons and positrons (Xu et al. 1999, 2001). However, the existence of BPCSSs is rather speculative and certainly not widely accepted. Possibility 3 seems to be a viable option. In fact, in the ultrahigh magnetic field the pairs are produced near the kinematic threshold $(\hbar\omega/2mc^2)h/\mathscr{R} \sim 1$ (Daugherty & Harding 1983). The near-threshold critical lines for the VG-ICS formation are described by the equation (15) in § 3. We can use $b = 100$ and $\mathscr{R}_6^{0.8}(k\mathscr{F})^{0.7} = 0.1$ to obtain the extremal critical line $\dot{P}_{-15} = 0.003P^{-2.2}$, which is presented as line 3 in Figure 1. Since the dipolar magnetic field in the considered region of the P-$\dot{P}$ diagram is low ($B_d \sim 10^{11}$ G), it is conceivable to increase the value of b to about few hundred (and still not to exceed $B_q \sim 4.4 \times 10^{13}$ G). Thus, it is obvious that all normal pulsar can be explained by a VG-ICS and/or VG-CR inner accelerator without invoking the BPCSS conjecture (Xu et al. 1999, 2001).

As one can see from Figure 1, the near-threshold ICS gap (line 3) makes an important difference from the near-threshold CR gap (line 2), which follows from the fact that in the ICS case the electron mean free path $l_e \sim h$ is important, while in the VG case $l_e \ll h$ it is negligible (Zhang et al. 2000). Moreover, in the asymptotic case the gap height $h \sim l_e$ is quite long (see eq. [13]), and the polar cap heating is considerable. However, since $l_e \propto B_s^{-1}$, the higher surface magnetic field B_s leads to much lower gap heights in the near-threshold case (see eq. [12]) and correspondingly lower surface temperatures T_s.

Our working hypothesis therefore is that the observed normal radio pulsars are driven by a VG inner accelerator. This means that $T_s/T_i < 1$ for pulsars located above the critical lines 1, 2, or 3. We further speculate that shorter or longer episodes of $T_s/T_i < 1$ (when the VG gap cannot form) could be attributed to the well-known and common phenomenon of pulse nulling. As Rankin (1986) demonstrated, nulling occurs simultaneously in both core and conal components of complex profiles, meaning that this phenomenon is associated with neither core nor conal emission. However, the core single pulsars apparently do not null. This striking property seems to have a natural explanation within the framework of our model. In fact, the core single pulsars occupy regions of the P-$\dot{P}$ diagram well above the critical lines for which $T_s = T_i$. Taking $P \sim 0.3$ s and $\dot{P}_{-15} \sim 30$ as the average values in the group of core single pulsars (see Fig. 6 in Gil & Sendyk 2000), we obtain from equation (17) that $T_s/T_i = 0.4$ even for $k\mathscr{F} = b = \mathscr{R}_6 = 1$, so the VG-CR gap can always form in these objects. We intend to explore the above mentioned idea in a separate paper.

5. PULSAR DEATH LINES AND PSR J2144−3933

In this section we examine an influence of strong surface magnetic fields required by the ion binding-energy problem on the location of death lines on the P-$\dot{P}$ diagram. We are especially interested in PSR J2144−3933 with the extremal period $P = 8.5$ s, which lies well beyond all conventional death lines. An approximate condition for pair creation in a strong magnetic field B was given by Erber (1966). In the limit of high photon energies $\hbar\omega \gtrsim 2mc^2$, the conversion rate depends sensitively on the parameter $\chi = (\hbar\omega/2mc^2)(h/\mathscr{R})(B/B_q) \gtrsim 1/15$. Cheng & Ruderman (1993) considered the problem of death lines in nondipolar configurations of the surface magnetic field at the pulsar polar cap using the asymptotic approximation described by the above condition $\chi \gtrsim 1/15$. We first apply their results to the new 8.5 s period pulsar. With very curved lines and a strong field, the gap height is $h \sim (B_d/B_s)^{1/2}R(2\pi R/cP)^{1/2}$. When this reduction of the gap height is taken into account, then the corresponding death line equation takes the form

$$\log B_d = 1.9 \log P - \log B_s + 0.6 \log \mathscr{R} + 21 ,$$

where we introduced the radius of curvature explicitly. Setting $P = 8.5$ s and $B_d = 4 \times 10^{12}$ G, we find that $B_s \gtrsim 10^{13}$ G and $\mathscr{R} \ll 10^6$ cm.

The above asymptotic considerations suggest that the surface magnetic field in PSR J2144−3933 should be very strong and extremely curved (see also Young et al. 1999). However, the asymptotic condition for magnetic pair creation is not valid for magnetic fields $B_s \gtrsim 0.1B_c \approx 5 \times 10^{12}$ G, which is much lower than surface fields inferred just above by means of this approximation. Thus, we have to use the near-threshold condition $\hbar\omega \sin\theta \gtrsim 2mc^2$, discussed generally in § 3. A general form of the near threshold death line is expressed by equation (11). For PSR J2144−3933, $P = 8.5$ s and $\dot{P}_{-15} = 0.475$, and thus we obtain a condition $\mathscr{R}_6^2 b^{0.5} = 0.13$. Treating this as a general condition, we obtain a death line $\dot{P}_{-15} = (3 \times 10^{-5})P^{4.5}$, which is presented as line 4 in Figure 1. Since in PSR J2114−3933, $B_d = 4 \times 10^{12}$ G (and $B_s = bB_d < B_q = 7.6 \times 10^{13}$ G), then $2 \lesssim b \lesssim 20$, which gives $0.3 \gtrsim \mathscr{R}_6 \gtrsim 0.17$.

It is also interesting to compare the near-threshold ICS-induced death line with the CR-induced death line represented by line 4 in Figure 1. Using equation (16) and putting $b = 100$ and $\mathscr{R}_6 = 0.1$ into it, one obtains the death line $\dot{P}_{-15} = 0.0002P^{-0.28}$, which is presented as line 5 in Figure 1. Obviously, this critical death line can explain all normal (nonmillisecond) pulsars. However, the case of PSR J2114−3933 can be interpreted with much less ad hoc field configuration, for example $b \approx 2$ and $\mathscr{R} \sim 1$.

6. CONCLUSIONS

In this paper we have examined an influence of an extremely strong and curved surface magnetic field on the long-standing binding-energy problem (for a review, see Xu et al. 1999). We have demonstrated within CR- and/or ICS-driven pair production models that the formation of a vacuum gap above the pulsar polar cap is possible in principle, provided that $B_s \gg B_d$ and $\mathscr{R} \ll R$. We have also addressed in this paper a very interesting and currently topical problem of why so many radio pulsars are beyond the conventional death lines, where theoretically they should not be converting high-energy photons into electron-positron pairs. PSR J2144−3933 is the pulsar of our special interest, with $P = 8.5$ s and $\dot{P} = 4.75 \times 10^{-16}$ (thus $B_d = 4 \times 10^{12}$ G), which is located extremely far beyond conventional death lines (circle in Fig. 1). Assuming a strong multipolar surface magnetic field suggested by the binding-energy problem, we can explain this extremal object without invoking any different radiation mechanism other than that for ordinary pulsars. Values of $B_s \gtrsim 10^{13}$ G and $\mathscr{R} \lesssim 10^5$ cm seem to fit the constraint imposed by the 8.5 s period well. Young et al. (1999) have noticed that an extremely twisted field could explain marginally the pulsar location in the B_d-P diagram, but they consider such fields unlikely. However, they did not consider a sunspot-like configuration that we use in this paper.

There is growing evidence that quite a large number of conal-type pulsars (Rankin 1986) with drifting subpulses (grazing cuts of the line of sight) or periodic intensity modulation (central cuts of the line of sight) have the RS75-type polar gap accelerators with curvature radiation–dominated magnetic pair production (Ruderman & Sutherland 1975; Deshpande & Rankin 1999; Vivekanand & Joshi 1999; Xu et al. 1999; Gil & Sendyk 2000). We argue in this paper that in such cases the surface magnetic field penetrating the polar gap should be dominated by strong multipolar (presumably sunspot-like magnetic field with $B_d \ll B \lesssim B_q$ and $\mathscr{R} \ll R$) components, reconnecting with a global dipole field well before the radio emission region. Zhang et al. (2000) concluded in their recent paper that it is not necessary to postulate ad hoc a multipolar field configuration to explain PSR J2144−3933. In fact, they demonstrated that the ICS-induced SCLF accelerator produces death lines that include PSR J2144−3993. However, we would like to strongly emphasize that the SCLF model is unable to explain the subpulse drift phenomenon, which seems to be a common phenomenon, at least among the conal-type profile pulsars (Rankin 1986; Gil & Sendyk 2000), although there is no direct evidence for conal-type emission in PSR J2144−3933.

As can be seen from Figure 1, the VG formation in principle is possible for all normal pulsars (excluding binary and millisecond ones, but see discussion in the next paragraph), provided that the surface magnetic field is extremely strong and curved. Pulsars above line 1 can form the VG-CR inner accelerator even with a relatively low surface field, $B_s \lesssim 5B_d$. However, pulsars below this line require much higher fields, $B_s \gg B_d$, to form the VG-CR accelerator ($b \sim 100$ at line 2, but it has to decrease toward line 1, since the actual field should not exceed the critical field $B_c \sim 5 \times 10^{13}$ G). Below line 2 one cannot form the VG-CR accelerator unless $B_s \gg 100B_d$. However, it is possible to form a VG-ICS inner accelerator with $b \sim 100$ and $\mathscr{R}_6 \sim 0.1$ on line 3. Since the dipolar field $B_d \sim 10^{11}$ G around this line, one can use b even larger than 100, and therefore all normal pulsars lie above critical lines for the VG formation. The general conclusion is that the VG formation, either CR- or ICS-induced, requires a strong and curved surface magnetic field with a radius of curvature $\mathscr{R} \sim 10^5$ cm and the field strength $B_c \gtrsim B_s \gg B_d$, where B_c is the photon-splitting level. This implies that radio pulsars (at least non-millisecond ones) are neutron stars with a surface magnetic field strength 5–100 times the surface dipolar component derived from P and $\dot{P}$ values. Such neutron stars can form VG-CR or VG-ICS inner accelerators, which discharge via a number of localized sparks. Both VG-CR and VG-ICS accelerators produce sparks, the importance of which for the mechanism of coherent pulsar radio emission was recently emphasized by Xu et al. (2001).

We have shown in this paper that VG formation in typical pulsars requires the crust-origin surface multipolar field to be much stronger (up to 100 times) than the dipolar surface component of the star-centered global field. In order to apply to the millisecond pulsars, we would have to invoke magnification factors of 10^4–10^5. This would mean that the millisecond pulsars have surface magnetic fields of the same order as the typical (normal) pulsars. Cheng, Gil, & Zhang (1998) came to a similar conclusion analyzing the nonthermal X-ray emission from outer gaps of rotation-powered pulsars. Whether such a strong surface magnetic field can exist in millisecond pulsars is not known. We would like to mention here one constraint found in the literature. Arons (1993) has shown that the location of the spin-up line in the P-$\dot{P}$ diagram constrains the large-scale anomalies of the magnetic field at the surface to no more than about 40% of the surface strength of dipolar field. This constraint does not concern the crust-origin small-scale anomalies invoked in this paper, which will not affect the dipolar structure of the magnetic field in the radio emission region. However, if such extremely strong fields are excluded in the millisecond pulsars, then their inner accelerator must be of SCLF type, which implies the maser kind of radio emission mechanism (Kazbegi et al. 1987, 1992).

The sparking discharge within a VG inner accelerator also is a natural explanation of the subpulse drift/periodic modulation. The group of pulsars with clearly drifting subpulses seem to favor the VG-CR model, although the VG-ICS model is not excluded. Few well-known drifters lying below line 2 in Figure 1 seem to require the ICS contribution or even domination of the gap discharge. It is important to emphasize that pulsars with signatures of periodic subpulse modulations seem to be distributed all over the bulk of the P-$\dot{P}$ plane (Rankin 1986). Therefore, it seems unlikely that pulsars with drifting subpulses represent the VG accelerator, while others are driven by the SCLF accelerator. We suggest that normal radio pulsars are those neutron stars that can develop the VG inner accelerator above their polar caps. This interpretation is consistent with the current status of theory of the coherent pulsar radio emission, which also seems to favor the sparking VG model, at least in normal pulsars (Gil & Sendyk 2000; Melikidze et al. 2000). The millisecond pulsars are probably driven by the SCLF inner accelerator. This problem will be examined in a forthcoming paper.

We would like to note that a sunspot-like configuration conjectured in this paper for VG formation and supported by the case of PSR J2144−3933 is also suggested by the spin-down index of PSR B0540−69 (Cheng & Ruderman 1993; Ruderman, Zhu, & Cheng 1998). Also, Cheng & Zhang (1999), analyzing the X-ray emissions from regions near the polar cap of the rotation-powered pulsars, argued that $B_s \sim 10^{13}$ G and $\mathscr{R} \sim 10^5$ cm, which agrees well with our independent estimates. As already mentioned, Gil & Sendyk (2000), attempting to explain morphological differences in pulse shapes and variations in polarization properties of different profile types as well as the subpulse drift rates, concluded that the surface magnetic field at the polar cap should be dominated by sunspot-like structures. It seems that there is growing evidence of such small-scale anomalies in the surface magnetic field of radio pulsars (see also Page & Sarmiento 1996; Ruderman 1991), and our paper gives independent arguments supporting this idea.

Polarization studies in radio pulsars seem to suggest that a significant part of the radio emission arises from regions in the magnetosphere where the magnetic field is largely dipolar. Also, studies concerning the morphology of pulse profiles are consistent with dipolar magnetic field structure in the radio emission altitudes, which are thought to be arising close to the stellar surface given by the relation $r \sim 50RP^{0.3}$ (Kijak & Gil 1997, 1998). Thus, if there are strong and complicated surface magnetic fields $B_s \sim 100B_d$ on the stellar surface, it is important to assess whether complicated fields would decay fast enough with altitudes such that in the emission region the magnetic field structure is almost purely dipolar as constrained by observations. On the other hand, the radius of curvature of surface field lines should be about 10^5–10^6 cm, which means that the structure of the gap magnetic field is determined by multipoles higher than the quadrupole. Here we consider the model of the magnetic field to be sunspot-like near the surface of the neutron star while the global dipolar magnetic field is that of a star-centered dipole. Such small-scale magnetic fields on the surface of the neutron star also have been considered by several authors to explain the radio emission properties from pulsars (see, e.g., Vivekanand & Radhakrishnan 1980; Krolik 1991). In the "crustal model" of the neutron star where the magnetic field is generated in the neutron star due to the currents in the crust, it is predicted that these models are only capable of producing small-scale magnetic fields (Urpin, Levshakov, & Yakovlev 1986). These small-scale fields can be modeled as small current loops giving rise to dipolar fields which are oriented in different directions all over the stellar surface and superposed on the global dipole field. Following this, one can express the magnetic field $B(r)$ at a distance r from the stellar center as the multipolar expansion $B(r) \approx B_d(R/r)^3 + \Sigma_{l \geq 3} B_l(R/r)^{l+1}$, where $l = 2, 3, 4, \ldots$ corresponds to dipole, quadrupole, octupole, etc., and B_l is the magnetic field strength of a given pole at the neutron star's surface. The number of reversals of the magnetic field across the stellar surface depends on the order of the multipole in question. For example, a pure dipolar field will have two reversals, while a pure quadrupole will have four reversals, and in general for a multipole of order l there will be 2^{l-1} reversals. Here we consider the multipolar field which has sunspot-like magnetic loops with a typical radius of curvature $\mathscr{R} \sim 0.1R \approx 10^5$ cm. This type of structure corresponds to multipoles of the order $l > 4$. The actual multipole order of a crust origin field clump can be estimated as $l \sim \Delta r/R$, where $\Delta r \sim 0.1R$ is a characteristic crust thickness. For typical pulsars with $P \sim 1$ s, the radio emission arises at altitudes $r \sim 50R$, and the ratio $B_d/B_{l>4} > 1$ in the emission region even if $B_l/B_d \sim 100$ at the surface. This means that radio emission arises from dipolar field lines even if there are strong, small-scale multipolar anomalies on the surface of the polar cap. The field surface strength of a local multipole is $B_s \sim (R/\Delta r)^m B_d$, where $m = 1$ or 2 depending on the relative orientation of adjacent magnetic moments (see, e.g., Arons 1993). This gives an estimate $B_s/B_d \sim 10$–100, as inferred in this paper using the binding-energy arguments.

It is worth emphasizing that all our conclusions presented in this paper concern vacuum gaps in neutron stars. Therefore, we claim that it may not be necessary to invoke the BPCSS conjecture proposed by Xu et al. (1999), according to which pulsars, at least those with drifting subpulses, are strange stars with bare polar caps (for review see Xu et al. 2000). However, we have to admit that we cannot exclude the BPCSS hypothesis.

A complicated magnetic field with a radius of curvature much smaller than the star radius has to be confined to the neutron star crust. Mitra, Konar, & Bhattacharya (1999) examined the evolution of multipole components generated by currents in the outer crust. They found that mostly low-order multipoles contribute to the required small radii of curvature and that the structure of the surface magnetic field is not expected to change significantly during the radio pulsar lifetime. The important question is if the crust can support surface magnetic fields with a magnitude approaching 10^{14} G. Equating the magnetic pressure of a strong multipolar field to the crustal stress, one concludes that the maximum field that the neutron star can sustain is approximately 10^{14}–10^{15} G (Thomson & Duncan 1995). Thus, our inferred magnitudes $B_s > 10^{13}$ G are in the regime where the cracking of the neutron star crust still will not occur.

We would like to point out a small weakness of our paper, namely, an apparent lack of pulsars in a valley between marginal line 4 in Figure 1 (including the extremal pulsar PSR J2144$-$3933) and the right-hand boundary of the bulk of the P-$\dot{P}$ distribution. The lack of pulsars at the long-period regime near the 8.5 s pulsar is understandable, since detectibility of long-period pulsars is much smaller than that of shorter ones, as pointed out by Young et al. (1999). The lack of shorter period pulsars within this valley has been explained by Zhang et al. (2000), who invoked a death line below which pair production is not supported by the SCLF-ICS mechanism (line IV in their Fig. 1). Within our VG scenario, this might just mean that strong multipole fields are possible but not common in old pulsars. Another possible explanation concerns a luminosity issue. Let us notice that PSR J2144$-$3933 is a very old (281 Myr), extremely weak (4 mJy), and close to the Earth (0.19 kpc) pulsar. It would probably not be detected if it was located just a bit farther away. So perhaps the radio luminosity of pulsars drops below a detection threshold of a typical survey before their inner accelerators stop completely producing a pair plasma.

Finally, we would like to emphasize once again that vacuum gaps, which we have shown to exist in pulsars, produce sparking discharges. These isolated sparks seem to be involved naturally with drifting subpulses observed in typical pulsars (see, e.g., Rankin 1986; Deshpande & Rankin 1999; Gil & Sendyk 2000). On the other hand, spark-associated models of the coherent pulsar radio emission (Melikidze et al. 2000) critically depend on the existence of nonstationary vacuum gaps, and therefore our paper supports these ideas on fundamental grounds.

This paper is supported in part by the grant 2 P03D 008 19 of the Polish State Committee for Scientific Research.

We are indebted to the referee B. Zhang for insightful comments and constructive criticism, which greatly helped to improve the final version of the paper. We are also thankful to K. S. Cheng, J. Kijak, D. Khechinashvili, G. Machabeli, G. Melikidze, B. Stappers, and B. Rudak for helpful comments and discussions. We also thank the Max-Planck-Institut für Radioastronomie and the Astronomical Institute "Anton Pannekoek" University of Amsterdam for kind hospitality, where part of this work was done. D. M. thanks J. Kepler Astronomical Center for support and hospitality during his visit to the institute, where this work was started. We thank E. Gil for technical assistance.

REFERENCES

Abrahams, A. M., & Shapiro, S. L. 1991, ApJ, 374, 652
Arons, J. 1993, ApJ, 408, 160
———. 2000, in IAU Colloq. 177, Pulsar Astronomy: 2000 and Beyond, ed. M. Kramer, N. Wex, & R. Wielebinski (ASP Conf. Ser. 202; San Francisco: ASP), 449
Arons, J., & Scharlemann, E. T. 1979, ApJ, 231, 854
Asseo, E., & Melikidze, G. I. 1998, MNRAS, 301, 59
Baring, G. M., & Harding, A. K. 1998, ApJ, 507, L55
Cheng, K., & Ruderman, M. A. 1977, ApJ, 214, 598
———. 1980, ApJ, 235, 576
———. 1993, ApJ, 402, 264
Cheng, K. S., Gil, J., & Zhang, L. 1998, ApJ, 493, L35
Cheng, K. S., & Zhang, L. 1999, ApJ, 515, 337
Cordes, J. M. 1992, in IAU Colloq. 128, The Magnetospheric Structure and Emission Mechanisms of Radio Pulsars, ed. T. H. Hankins, J. M. Rankin, & J. Gil (Zielona Góra: Pedagogical Univ. Press), 253
Daugherty, J., & Harding, A. K. 1983, ApJ, 273, 761
Deshpande, A. A., & Rankin J. M. 1999, ApJ, 524, 1008
Eichler, D., & Cheng, A. F. 1989, ApJ, 336, 360
Erber, T. 1966, Rev. Mod. Phys., 38, 626
Gangadhara, R. T., et al. 1999, A&A, 342, 474
Gil, J. 1992, A&A, 256, 495
Gil, J., & Sendyk, M. 2000, ApJ, 541, 351
Goldreich, P., & Julian, H. 1969, ApJ, 157, 869
Hillebrandt, W., & Müller, E. 1976, ApJ, 207, 589
Kazbegi, A. Z., Machabeli, G. Z., & Melikidze, G. I. 1992, in IAU Colloq. 128, The Magnetospheric Structure and Emission Mechanisms of Radio Pulsars, ed. T. H. Hankins, J. M. Rankin, & J. Gil (Zielona Góra: Pedagogical Univ. Press), 232
Kazbegi, A. Z., Machabeli, G. Z., Melikidze, G. I., & Usov, V. V. 1987, Australian J. Phys., 40, 755
Kijak, J., & Gil, J. 1997, MNRAS, 288, 631
———. 1998, MNRAS, 299, 855
Kössl, D., Wolff, R. G., Müller, E., & Hillebrandt, W. 1988, A&A, 205, 347
Krolik, J. 1991, ApJ, 373, L69
Melikidze, G. I., Gil, J., & Pataraya, A. D. 2000, ApJ, 544, 1081
Mitra, D., & Deshpande, A. A. 1999, A&A, 346, 906
Mitra, D., Konar, S., & Bhattacharya, D. 1999, MNRAS, 307, 459
Muslimov, A. G., & Tsygan, A. I. 1992, MNRAS, 255, 61
Page, D., & Sarmiento, A. 1996, ApJ, 473, 1067
Qiao, G. J., & Lin, W. P. 1998, A&A, 333, 172
Rankin, J. M. 1986, ApJ, 301, 901
Ruderman, M. A. 1991, ApJ, 366, 261
Ruderman, M. A., & Sutherland, P. G. 1975, ApJ, 196, 51 (RS75)
Ruderman, M. A., Zhu, T., & Cheng, K. 1998, ApJ, 492, 267
Sturrock, P. A. 1971, ApJ, 164, 529
Taylor, J. H., Manchester, R. N., & Lyne, A. G. 1993, ApJS, 88, 529
Thompson, C., & Duncan, R. 1995, MNRAS, 275, 255
Urpin, V. A., Levshakov, S. A., & Yakovlev, D. G. 1986, MNRAS, 219, 703
Usov, V. V., & Melrose, D. B. 1995, Australian J. Phys., 48, 571
Vivekanand, M., & Joshi, B. C. 1999, ApJ, 515, 398
Vivekanand, M., & Radhakrishnan, V. 1980, J. Astrophys. Astron., 1, 119
Xu, R. X., Liu, J. F., Han, J. L., & Qiao, G. J. 2000, ApJ, 535, 354
Xu, R. X., Qiao, G. J., & Zhang, B. 1999, ApJ, 522, L109
Xu, R. X., Zhang, B., & Qiao, G. J. 2001, Astropart. Phys., 15(1), 101
Young, M. D., Manchester, R. N., & Johnston, S. 1999, Nature, 400, 848
Zhang, B., Qiao, G. J., & Han, J. L. 1997a, ApJ, 491, 891
Zhang, B., Qiao, G. J., Lin, W. P., & Han, J. L. 1997b, ApJ, 478, 313
Zhang, B., & Harding, A. K. 2000a, ApJ, 532, 1150
———. 2000b, ApJ, 535, L51
Zhang, B., Harding, A. K., & Muslimov, A. 2000, ApJ, 531, L135